Eur. Phys. J. D **23**, 201–209 (2003)
DOI: 10.1140/epjd/e2003-00032-x

THE EUROPEAN PHYSICAL JOURNAL D

Barkas effect, shell correction, screening and correlation in collisional energy-loss straggling of an ion beam

P. Sigmund[1] and A. Schinner[2]

[1] Physics Department, University of Southern Denmark, 5230 Odense M, Denmark
[2] Institut für Experimentalphysik, Johannes-Kepler-Universität, 4040 Linz-Auhof, Austria

Received 24 September 2002 / Received in final form 1st December 2002
Published online 4 February 2003

Abstract. Collisional electronic energy-loss straggling has been treated theoretically on the basis of the binary theory of electronic stopping. In view of the absence of a Bloch correction in straggling the range of validity of the theory includes both the classical and the Born regime. The theory incorporates Barkas effect and projectile screening. Shell correction and electron bunching are added on. In the absence of shell corrections the Barkas effect has a dominating influence on straggling, but much of this is wiped out when the shell correction is included. Weak projectile screening tends to noticeably reduce collisional straggling. Sizable bunching effects are found in particular for heavy ions. Comparisons are made with selected results of the experimental and theoretical literature.

PACS. 34.50.Bw Energy loss and stopping power – 52.40.Mj Particle beam interactions in plasmas

1 Introduction

In 1915, Bohr [1] predicted that the fluctuation of the energy loss ΔE of a beam of charged particles penetrating matter is characterized by the variance

$$\left\langle (\Delta E - \langle \Delta E \rangle)^2 \right\rangle = NRW \tag{1}$$

with the straggling parameter W given by

$$W = W_{\mathrm{B}} = 4\pi Z_1^2 Z_2 e^4, \tag{2}$$

where $\langle \Delta E \rangle$ is the mean energy loss over a travelled pathlength R, N the number of atoms per volume in the stopping material, and Z_1, Z_2 the atomic numbers of beam and material atoms, respectively.

Equation (1) assumes the stopping medium to be random and the pathlength R sufficiently small so that the variation with beam energy of the cross-sections responsible for energy loss can be ignored [2,3].

Equation (2) assumes free-Coulomb scattering between beam particles and the electrons of the stopping medium. Bohr showed that unlike the mean energy loss, straggling is rather insensitive to the binding of target electrons. The underlying reason is the fact that the integral

$$W = \int T^2 \mathrm{d}\sigma(T) \tag{3}$$

is dominated by large values of the energy transfer T per collision event even though the differential cross-section $\mathrm{d}\sigma(T)$ is heavily peaked toward small T.

Equation (2), in conjunction with (1), seems to constitute one of the most lasting and universally-valid results of the theory of particle penetration. Its range of validity reaches far beyond the initial application area, *i.e.*, α-particles from radioactive sources. Nevertheless there are limitations which, according to common knowledge, may roughly be classified into three groups,

1. at low projectile speed, comparable to electron velocities in the target, W tends to slightly increase above the Bohr value with decreasing velocity before dropping toward zero [4],
2. at high speed, relativistic corrections beyond those mentioned already by Bohr [1] become necessary [5] and
3. charge exchange may not be neglected in general as a source of energy-loss straggling [6].

This paper addresses the first group of phenomena which is well separated from the second group because of non-overlapping velocity regimes. Phenomena of the third group need to be considered in comparisons with experiment, but their theoretical study involves different physics [7–11] and will be left out here.

Physical effects potentially causing deviations from free-Coulomb scattering at low projectile speed are primarily those that also affect the stopping force,

- binding of target electrons,
- orbital motion of target electrons,
- Barkas effect,
- projectile screening by accompanying electrons,
- interplay between Born approximation and classical-orbit description of ion-electron scattering.

Additionally for straggling,

- correlation between target electrons may be contributing and
- high-energy-transfer processes like electron promotion may become noticeable even if insignificant in the stopping force [12].

Although there have been made estimates of energy-loss straggling at moderate and low projectile velocities [13–16], we are unaware of systematic attempts to identify contributions from the physically distinct processes listed above. In particular, information on the influence of the Barkas effect on straggling has been emerging only recently [11] even though its contribution to the stopping force has been studied extensively.

The binary theory of electronic stopping [17] has proven to be a useful tool in the computation of stopping forces over a wide range of ions and energies above, around and below the stopping maximum. Good quantitative agreement has been achieved with experimental data for numerous ion-target combinations [18]. The adopted energy-loss mechanism is Coulomb excitation of target electrons.

We aim at treating the effects of electron binding, orbital motion, Barkas effect, projectile screening and correlation down to velocities $v \sim v_0$ or $E \sim 0.025$ MeV/u. Stopping forces can be predicted down to ~ 1 keV/u, but with an increased error margin. Neither Z_1 oscillations nor electron-promotion effects are contained in the scheme. This, as well as the fact that only limited experimental data are available for test purposes, suggests caution with regard to predictions of straggling below v_0, based upon this scheme.

2 Theoretical scheme

The basics of binary stopping theory have been described in references [17,19], and an extensive documentation on the computation of stopping forces including several add-ons has appeared recently [18]. The purpose of the present section is to add specific features pertinent to straggling.

The fundamental quantity in the binary theory is a classical energy-loss function $T(p,\omega_j)$ characterizing the energy transfer by Coulomb interaction from a screened projectile ion moving at an impact parameter p past a target electron bound harmonically by a frequency ω_j. This function is calculated nonperturbatively. It approaches the free-Coulomb limit at small p and the Bohr function [20] at large p.

From this we may obtain an expression for the straggling parameter per target electron,

$$W_{0j} = \int_0^\infty 2\pi p \,\mathrm{d}p \,\left[T(p,\omega_j)\right]^2, \tag{4}$$

from which one could obtain an expression for the straggling parameter of an atom,

$$W_0 = \sum_j Z_2 f_j W_{0j} \tag{5}$$

where $Z_2 f_j$ is the number of target electrons in the jth shell and $\sum_j f_j = 1$.

Equation (5) assumes target electrons to be statistically independent. The effect of correlations between target electrons will be discussed in Section 5. Screening and Barkas effect are contained in equation (4), whereas allowing for shell corrections is a second step involving kinetic theory [21] which, for binary elastic scattering, provides exact relationships between stopping parameters for a projectile moving through a medium with internal motion and the corresponding parameters for a medium at rest. For the straggling parameter this relation reads [21]

$$W_j = \left\langle \frac{1}{v|\mathbf{v}-\mathbf{v}_e|^3} \left[\left(\frac{3}{2}\left(v^2 - \mathbf{v}\cdot\mathbf{v}_e\right)^2 - \frac{1}{2}\left(\mathbf{v}-\mathbf{v}_e\right)^2 v^2 \right) W_{0j}\left(|\mathbf{v}-\mathbf{v}_e|\right) + \left(v^2 v_e^2 - \left(\mathbf{v}\cdot\mathbf{v}_e\right)^2 \right) \times m\left(\mathbf{v}-\mathbf{v}_e\right)^2 S_{0j}\left(|\mathbf{v}-\mathbf{v}_e|\right) \right] \right\rangle_j, \tag{6}$$

where $\mathbf{v}_e$ represents the velocity vector of the target electron and S_{0j} the stopping cross-section ignoring shell correction. The average is taken over the velocity distribution of the jth target shell. This leads to the straggling parameter of an atom,

$$W = \sum_j Z_2 f_j W_j. \tag{7}$$

Unless stated otherwise, calculations to be reported below refer to equation (5) ("no shell correction") or equation (7) ("shell correction included").

3 Bare ions

We first consider stopping of bare ions. While shell corrections may be switched on or off *via* equations (5, 7), the Barkas effect is an inherent part of the scheme which can be eliminated only by taking the average between output for a projectile and its antiparticle.

3.1 H-Si

Figure 1 shows relative straggling, *i.e.* the ratio W_0/W_B ignoring shell correction for protons and antiprotons in silicon as well as the average between the two quantities. In accordance with previous experience the average curve, *i.e.* the straggling parameter uncorrected for the Barkas effect, barely shows a Bethe-Livingston shoulder. For protons a pronounced shoulder is found which must be caused by the Barkas effect and is evidently unrelated to the Bethe-Livingston effect.

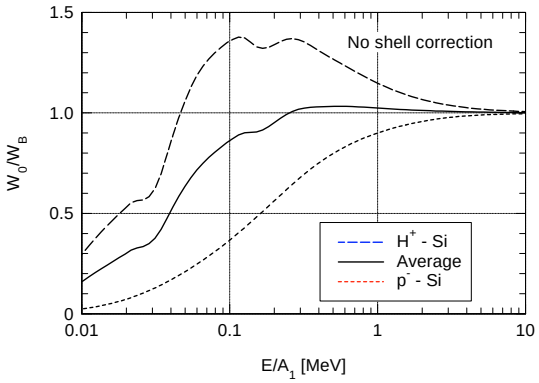

Fig. 1. Relative straggling W_0 (shell correction switched off) for protons and antiprotons in silicon and average.

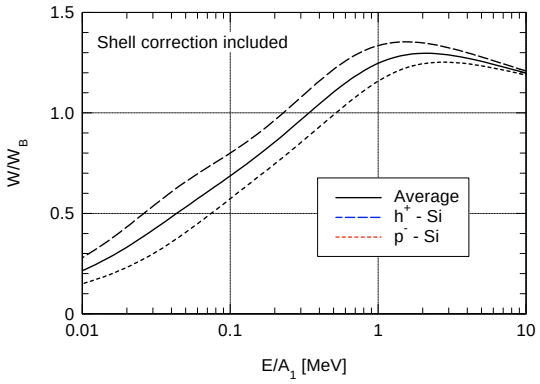

Fig. 3. Same as Figure 1 but shell correction switched on.

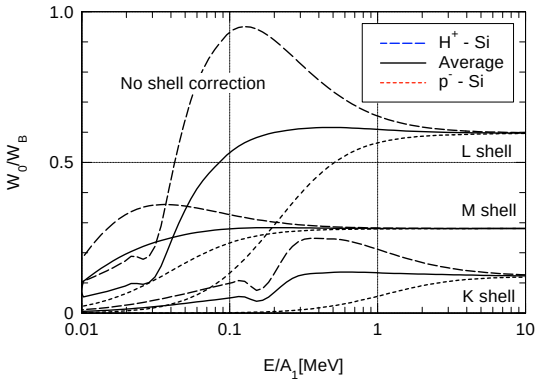

Fig. 2. Same as Figure 1 differentiated into target shells.

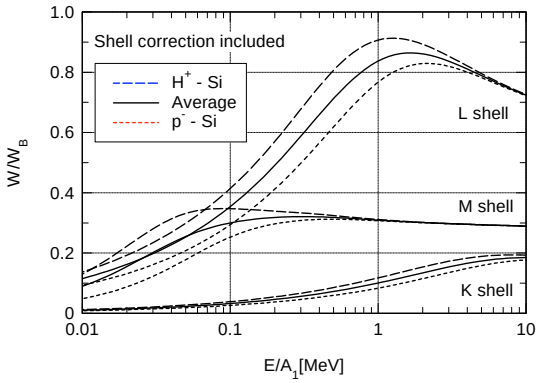

Fig. 4. Same as Figure 2 but shell correction switched on.

Figure 2 illustrates details, including the origin of the nonmonotonic behavior in Figure 1. The dominating cause is the fact that the K, L and M target shells have their individual shoulders at 0.35, 0.13, and 0.038 MeV/u, respectively. In addition one identifies small troughs which are artifacts arising from classical resonance scattering on an attractive screened-Coulomb potential [18]. Characteristically for the Barkas correction, the shoulder is most pronounced on a relative scale for the K shell even though the L shell dominates on an absolute scale due to the presence of more electrons.

We may conclude that in the absence of shell corrections the Barkas effect causes a dramatic difference between straggling parameters for protons and antiprotons.

Figure 3 shows the same system but now with the shell correction included. Consider first the curve labelled "Average" which represents bare protons without a Barkas correction. In accordance with conventional theory [4,22] a pronounced shoulder is now observed at 2.1 MeV/u, *i.e.*, at an energy about an order of magnitude higher than what was found for the Barkas effect. This shoulder is caused by orbital motion of target electrons, the velocity distribution of which is considerably broader than the width of the shoulder observed without shell correction in Figure 1. Therefore, that shoulder is essentially wiped out by the shell correction.

Note in particular that the effect of the shell correction is more pronounced in the stopping of protons than of antiprotons. This feature becomes particularly visible in Figure 4 which differentiates between target shells. Here the K shell experiences a shell correction with a shoulder around 10 MeV/u which completely wipes out the shoulder at 0.35 MeV/u generated by the Barkas effect. Conversely, for the M shell, orbital motion does not give rise to a noticeable shoulder, as is seen from the curve labelled "Average". Therefore, the shoulder observed for M-shell straggling of protons in Figure 4 must be caused by the Barkas effect. The effect of this can be seen in Figure 3 below 0.1 MeV/u, but it is very weak.

We may conclude that the Bethe-Livingston shoulder seen in Figure 3 originates in shell corrections to the K and L shell, that the observed Barkas splitting around the shoulder is mainly due to the L shell, and that the M shell gives rise to noticeable Barkas splitting but no pronounced shoulder around and below 0.1 MeV/u.

3.2 H-C and Li-C

Figure 5 shows a similar behavior for hydrogen in carbon. The main quantitative difference is a movement of the Bethe-Livingston shoulder toward lower velocities in accordance with the Z_2 dependence of the shell correction.

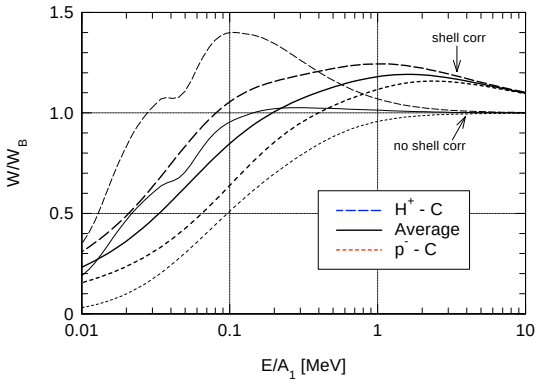

Fig. 5. Relative straggling for protons and antiprotons in carbon as well as average. Thick lines: shell correction included; thin lines: no shell correction.

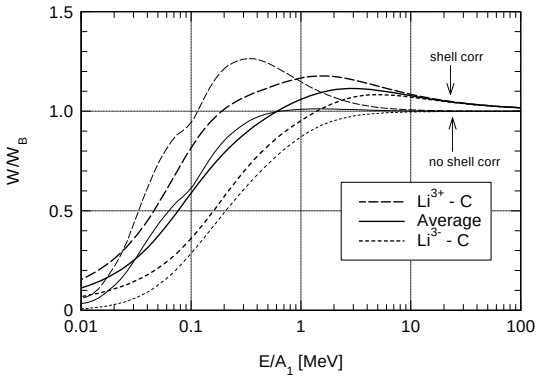

Fig. 6. Relative straggling for bare lithium and antilithium ions in carbon as well as average.

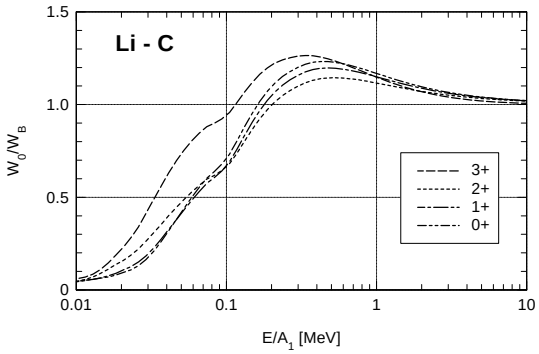

Fig. 7. Relative straggling for lithium in carbon (shell correction switched off) for frozen charge states 3+ to 0.

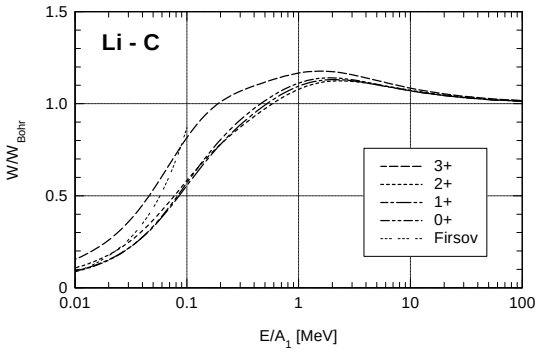

Fig. 8. Same as Figure 7 but shell correction switched on.

Figure 6 shows similar information for lithium in carbon. In curves denoted "Average" the Barkas effect has been eliminated by averaging between lithium and antilithium. In comparison with H–C the shoulder caused by the Barkas effect has moved further up in energy than the one caused by the shell correction in accordance with the Z_1 dependence of the Barkas effect. It now gives rise to a noticeable increase in the shoulder adding up to the Bethe-Livingston effect. However, the practical significance of this result is limited since the effect of projectile screening is essential at energies $\lesssim$0.1 MeV/u, as will be seen below.

3.3 Bloch correction

The results quoted above were obtained from a classical-orbit description of the scattering of a target electron on the projectile. The upper limit of validity of such a description is defined by the Bohr criterion [2]

$$v < 2Z_1 v_0 \tag{8}$$

or $E < Z_1^2 \times 0.1$ MeV/u. All graphs shown above go beyond that limit.

Bloch's stopping theory [23] provides the link between the classical Bohr model and Bethe's quantal perturbation theory [24]. In binary stopping theory, the range of validity of the classical model has been extended into the Bethe regime by addition of an inverse-Bloch correction [25,26].

Lindhard and Sørensen [5] recently provided a substantial extension of the Bloch theory. Essential in the present context is their discussion of straggling in the nonrelativistic regime. It was demonstrated that in the absence of Barkas and shell corrections there is no Bloch correction to the straggling parameter. Therefore, unlike in case of the stopping cross-section, no inverse-Bloch correction is necessary in straggling to extend the range of validity of the binary theory into the Bethe regime.

An expression for the straggling parameter was in fact evaluated from the Bloch theory by Titeica [27] which adds an extra term to the Bohr value. It was demonstrated in reference [21] that this additional term is a shell correction and as such derivable from kinetic theory. There is, therefore, no contradiction between the results of references [5,27].

4 Dressed ions

Figures 7 and 8 show relative straggling for frozen-charge Li ions in carbon with the shell correction switched off and on, respectively. The curves labelled "3+" were

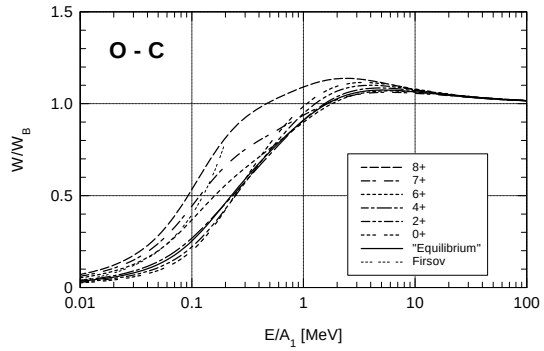

Fig. 9. Relative straggling for oxygen in carbon (shell correction switched on) for frozen charge states 8+ to 0. The curve labelled "equilibrium" is explained in the text.

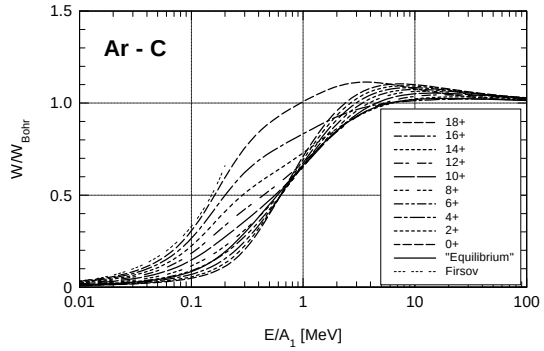

Fig. 10. Same as Figure 9 for argon in carbon.

already part of Figure 6[1]. It is seen that screening affects the shape of the straggling parameter below the shoulder region, both for the shoulder generated by the Barkas effect in Figure 7 and by the shell correction in Figure 8. The actual degree of screening appears to have surprisingly little influence.

In this and several of the following figures a curve labelled "Firsov" has been included for orientation which reflects Hvelplund's [29] evaluation of Firsov's energy-loss formula for single collisions [30]. Apart from the fact that Firsov's formula was not designed for this purpose by its author, it is a low-energy formula for $v \lesssim v_0$.

Figures 9 and 10 show oxygen and argon in carbon for different frozen charge states. Again the fully-stripped ion experiences significantly larger straggling than the screened ones although some dependence is now seen also for lower charge states.

[1] Somewhat surprisingly, Figure 7 indicates that $W/W_{\rm B}$ does not behave monotonically as a function of charge state in the region above the shoulder. This feature is related to the Barkas effect and was found to be quite pronounced in impact-parameter-dependent stopping under channeling conditions [28]. Inclusion of the shell correction (Fig. 8) reduces the effect to below the error of the Bohr model, the binary theory, and of even quite accurate straggling measurements. We shall therefore refrain from following up this feature here and now.

The equilibrium value of collisional straggling is given by [9]

$$W_{\rm equil} = \sum_J P_J W(q_J), \tag{9}$$

where P_J denotes the equilibrium occupation of charge state q_J. In applications of binary stopping theory, the corresponding expression for the stopping cross-section has most often been replaced by $S(\langle q\rangle)$ with

$$\langle q\rangle = \sum_J P_J q_J, \tag{10}$$

i.e. the stopping cross-section for an ion in the average charge state. If the same is done for straggling, *i.e.*

$$W_{\rm equ} \simeq W(\langle q\rangle) \tag{11}$$

one obtains the curve labelled "equilibrium" in Figures 9, 10 and 11. Since the curves for low charge states are close to each other, also the shape of the average is not sensitive to the way how the average is taken. Hence this curve can well be utilized to estimate collisional straggling in charge equilibrium within the accuracy of present-day experiments[2].

Figure 11 has been included because of the importance of these systems (He, B and P in Si) in ion implantation and analysis. Qualitative trends are very similar to what was found for carbon, but the variation with charge state appears to be less pronounced for the heavier target. This is a consequence of the competition between screening radius and adiabatic radius [31]: the higher I-value of Si causes a smaller adiabatic radius compared to the carbon target and hence a smaller influence of screening on the stopping integral.

5 Correlation

Correlations in straggling have been analysed in various contexts [3,15,22,32]. In a classical impact-parameter picture the straggling parameter per target atom may be written as

$$\begin{aligned} W &= \int \mathrm{d}^2\mathbf{p} \left\langle \left(\sum T_i(\mathbf{p}_i)\right)^2 \right\rangle \\ &= \int \mathrm{d}^2\mathbf{p} \sum_{i,j} \left\langle T_i(\mathbf{p}_i) T_j(\mathbf{p}_j) \right\rangle, \end{aligned} \tag{12}$$

where $T_i(\mathbf{p}_i)$ is the energy loss to the ith target electron at an impact parameter $\mathbf{p}_i$ and $\mathbf{p}$ the impact parameter

[2] The reader may note that the curve labelled "equilibrium" does not seem to coincide completely with the curve labelled 0+ in the velocity regime where the ion is essentially neutral. This feature is due to the shell correction in combination with equation (11) because the shell correction mixes contributions from higher and lower velocities. This does not occur if the correct expression (9) for equilibrium straggling is used.

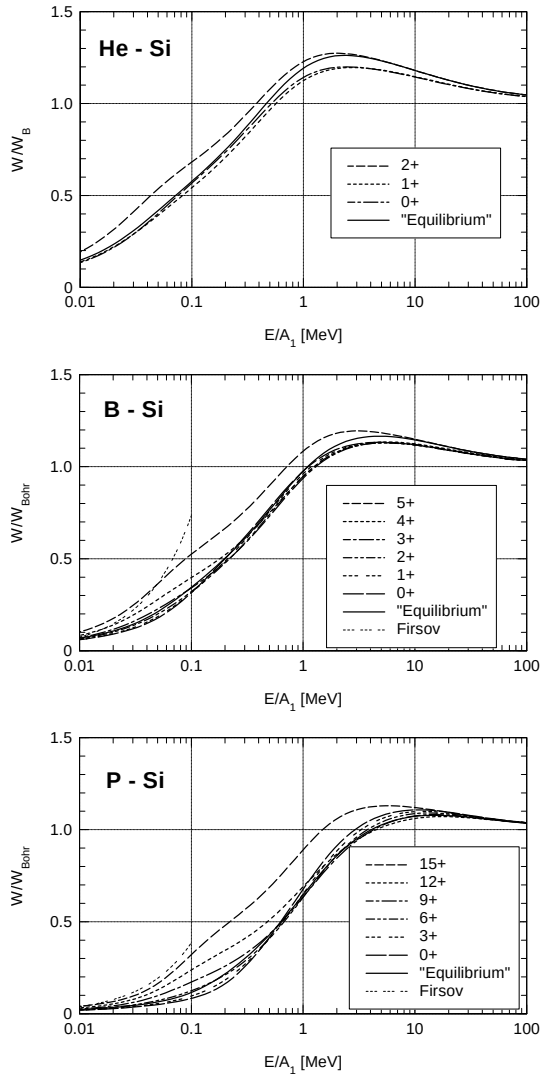

Fig. 11. Relative straggling for He, B and P ions in Si for several frozen charge states. For curves marked "equilibrium" see text.

with respect to the nucleus. The average is taken over the spatial distribution of target electrons around the nucleus.

We may split the sum into one part with $i = j$ which reduces to the one-electron straggling parameter equation (5) or (7) that has been evaluated already, and a correlation term reading

$$\Delta W = \int \mathrm{d}^2 p \sum_{i \neq j} \Big\langle T_i(\mathbf{p}_i) \Big\rangle \Big\langle T_j(\mathbf{p}_j) \Big\rangle, \qquad (13)$$

where the average has been factorized, assuming that the internal motion of target electrons can be approximated as uncorrelated. The term ΔW is nevertheless called a correlation term because it hinges on the spatial proximity of two target electrons in an atom.

The quantity

$$\langle T_i(\mathbf{p}_i) \rangle = \int \mathrm{d}^3 r_i |\psi_i(\mathbf{r}_i)|^2 T_i(\mathbf{p} - \boldsymbol{\rho}_i) \equiv T_i'(p) \qquad (14)$$

represents the mean energy transferred to the ith electron as a function of p, the impact parameter to the target nucleus. Here, $\psi_i(\mathbf{r}_i)$ is a single-particle wave function of a target electron and $\boldsymbol{\rho}_i$ the component of the electron coordinate $\mathbf{r}_i$ perpendicular to the projectile velocity. The difference between T_i and T_i' is substantial: T_i depends on the impact parameter to a target *electron* and hence approaches $2mv^2$ – or a shell-corrected maximum energy transfer – at $p = 0$. Conversely, T_i' may well have a minimum at $p = 0$ because the chance of hitting a target electron head-on is greater at a nonvanishing distance from the nucleus.

With this we may write

$$\Delta W = \int \mathrm{d}^2 p \Big(\sum_i T_i'(p) \Big) \Big(\sum_j T_j'(p) \Big) - \int \mathrm{d}^2 p \sum_i \Big(T_i'(p) \Big)^2 . \qquad (15)$$

Here, $\sum_i T_i'(p) \equiv T'(p)$ is the average energy transfer to the atom at an impact parameter p to the nucleus.

Equation (15) but without the second term was found by Besenbacher *et al.* [15] on the basis of an electron-gas model. We note that the second term is essential since in its absence also a one-electron atom would show correlation.

However, since the second term decreases in significance with increasing number of target electrons it is tempting to simplify the evaluation. For helium as a target which has only one shell, the integrand reads $4(T_K'(p))^2 - 2(T_K'(p))^2 = 2(T_K'(p))^2$, *i.e.*, the second term in equation (15) has half the magnitude of the first one. This has been taken into account in Figure 12. For the heavier targets we drop the second term but compensate approximately by applying a factor of $1 - 1/Z_2$ to the first term. This leads to the correct result for $Z_2 = 1$ and 2. An explicit evaluation for Ar in Si resulted in a ratio $\simeq 0.1$ between the second and the first term, almost independent of energy while the above estimate yields 0.07. This difference is well within the overall error of the present theory.

Figure 12 shows values of $\Delta W/W_\mathrm{B}$ calculated in this way for He and Ar ions in He, C and Si targets. In accordance with previous experience [33] the correction goes through a maximum near the maximum of the stopping force, and its magnitude increases with increasing Z_2, although this increase is less than linear around the maximum. The absolute magnitude is greater for Ar ions than for He at least around the maximum, and the absolute magnitude for He–He is consistent with the estimate in reference [15].

It was found in reference [15] that the correlation effect may have comparable magnitude as charge-exchange straggling. In view of a similar dependence on ion energy the two effects may be difficult to separate. While our findings are consistent with this, we need to add a word of caution about the absolute magnitude of the present

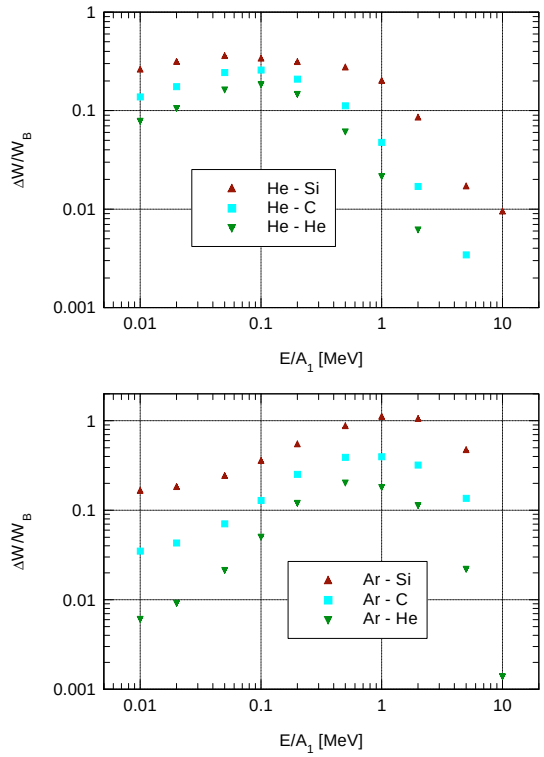

Fig. 12. Correlation term in straggling. See text.

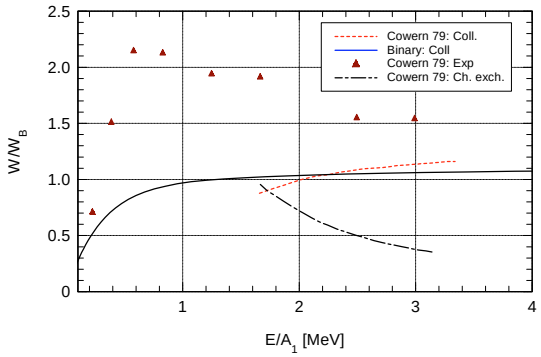

Fig. 13. Relative straggling for C–Al according to Cowern *et al.* [35]. Solid line: collisional straggling from binary theory excluding correlation. See text.

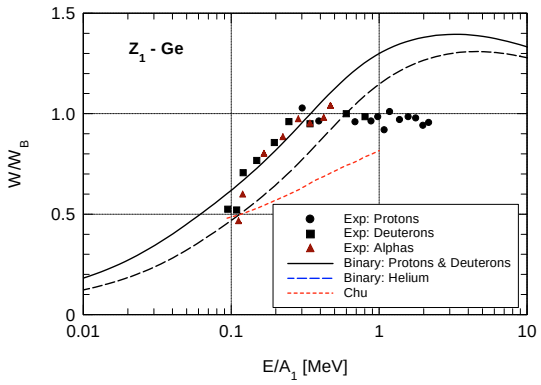

Fig. 14. Relative straggling for H, D and He in Ge. Experimental data from: [36]. Predictions of the binary theory and of [14].

estimates which appear high, especially for argon ions,

- most of all, target electrons have been treated as independent both in the intrinsic atomic motion and in the excitation process. Now, for a helium target the intrinsic motion of the two electrons is known to be anticorrelated to a certain extent. This gives rise to less straggling, although it is not obvious how to incorporate this into the present scheme;
- conversely, for heavy ions the excitation process is known to be correlated [34]. That this is affects stopping forces is one major reason for the present limitation to $Z_1 \lesssim 18$ in applications of the binary theory. This is possibly even more influential in straggling;
- also the combination of average ion charge and shell correction mentioned in the footnote on page 205 may be assumed to act here and to cause the somewhat peculiar low-velocity behavior for argon ions.

In summary, results of this paragraph are expected to express tendencies but are considered less quantitative than what was found for the previous effects. These results will not be incorporated into the estimates shown in the following section.

6 Discussion

Figure 13 shows experimental straggling data from Cowern *et al.* on carbon in aluminium. FWHM straggling data given in reference [35] have been converted into W/W_B assuming Gaussian profiles. The solid line shows collisional straggling calculated from the binary theory ignoring correlation. This curve agrees closely in the overlap region with the evaluation of the Bethe-Livingston formula given in reference [35]. Cowern *et al.* showed that the difference between their data and the Bethe-Livingston curve was consistent with an estimate of charge exchange straggling based on reasonable cross-sections for charge exchange.

Figure 14 shows relative straggling for protons, deuterons and alpha particles in germanium. The experimental data from reference [36] are similar to numerous data on other systems reported by the same group (*cf.* [37] and references quoted there). Those results were compared to the prediction of Chu [14]. Results from binary theory have been added here. While there is found better agreement between experiment and binary theory than with Chu's prediction at the low-energy end, the absence of a Bethe-Livingston shoulder in the experimental data is striking.

This feature is met frequently in the literature but is not universal. Shoulders were found *e.g.* in reference [15]. We note that experimental setups for measurement of energy-loss spectra frequently operate with a very narrow acceptance angle of the detector. Since straggling is predominantly due to close encounters, a significant fraction of ions contributing to electronic straggling could remain

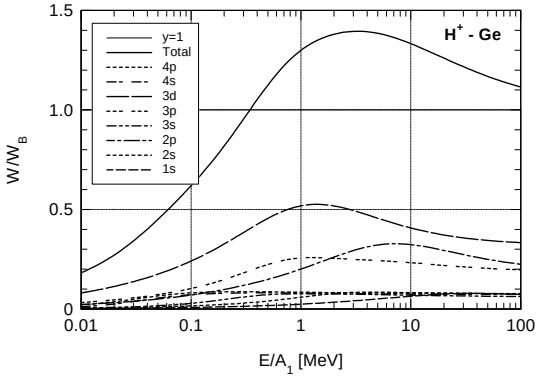

Fig. 15. Relative straggling of protons in Ge. Contributions from individual target shells.

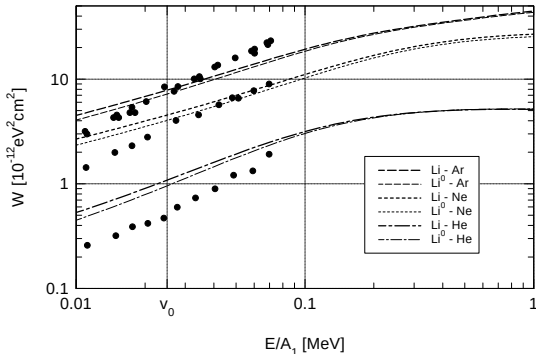

Fig. 16. Straggling for Li ions in noble gases: calculations disregarding correlation effect compared with measurements of Andersen *et al.* [38].

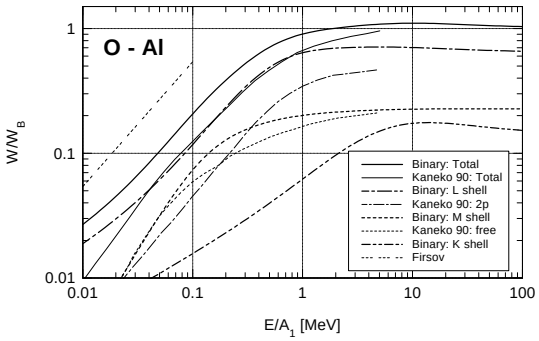

Fig. 17. Relative collisional straggling for O–Al, Contribution from individual shells. Binary theory ignoring correlation, and prediction of Kaneko [39].

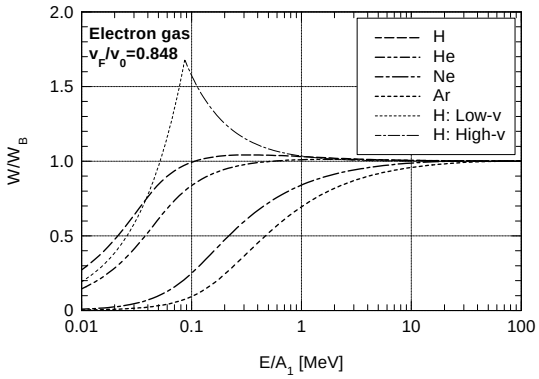

Fig. 18. Relative straggling for H, He, Ne and Ar ions in free electron gas equivalent with the average electron density of metallic lithium. Equilibrium charge state assumed. Low- and high-v expansions reflect expansions mentioned in reference [40].

undetected because of single and multiple elastic scattering on the target nucleus.

Figure 15 shows contributions to straggling from eight target shells in Ge. It is seen that the Bethe-Livingston shoulder is essentially made up by $2p$ and $3d$ electrons. The corresponding shell radii are 0.066 and 0.148 Å, respectively. At the point of bend-over, $\simeq 0.4$ MeV/u, Rutherford's law predicts scattering angles of 1 and 0.5 degrees at impact parameters 0.066 and 0.148 Å for both protons and α particles. According to available information, the experimental setup underlying reference [36] allowed for detection of particles scattered at somewhat larger angles. Hence, this effect may not constitute a full explanation for the absence of shoulders.

Figure 16 shows a comparison with measurements of Andersen *et al.* for lithium ions in He, Ne and Ar [38]. Data for other gases were left out of the comparison: for molecular gases the correlation effect complicates the matter, and for krypton and xenon our database is not yet adequate. Quite good agreement is found for Li–Ar and Li–Ne above v_0, while the theory appears to overestimate straggling for the Li–He system. While caution has been expressed above with regard to the applicability of the theory at such low velocities, the fact that the theory seems to *overestimate* straggling appears provoking.

Figure 17 shows a comparison with theoretical predictions of Kaneko [39] based on a free-electron-gas model. The prediction of the binary theory for the total straggling effect lies higher by up to about a factor of two. Only part of this can be caused by the missing Barkas effect in reference [39]. It seems that the contribution from $2s$ electrons was neglected altogether. The results for the M shell agree well at low and high velocities, and the difference at intermediate velocities may be ascribed to the Barkas effect. Figure 17 indicates that the discrepancy originates in the L shell, where an electron-gas model without a Barkas correction cannot be expected to be adequate.

Figure 18 shows results for a free-electron gas with the average electron density of metallic lithium corresponding to a density parameter $\chi^2 = v_0/\pi v_F = 0.375$. Results for hydrogen are compared with the low- and high-velocity expansions of reference [40]. It is seen that the binary theory yields a much less pronounced shoulder than an uncritical extrapolation of those expansions, in agreement with results of reference [13]. In that work the shoulder region was evaluated numerically without series expansion in v or $1/v$, and shoulder maxima of less than 1.1 were found.

7 Concluding remarks

In our opinion the main achievement of this work is insight into the role of the Barkas effect in straggling and a clarification of its interplay with the shell correction and projectile screening. The role of screening has been studied previously [16,39,41,42], and numerous investigations were devoted to shell corrections in straggling, but the Barkas effect has been a major hurdle especially in heavy-ion stopping and straggling.

Figures 1–6 indicate that consideration of the Barkas effect without simultaneous consideration of the shell correction may be misleading and tends to overestimate the magnitude of the correction.

Screening, on the other hand, reduces the overall interaction and hence also straggling, but somewhat surprisingly the major part of this reduction requires comparatively little screening, as is seen from Figures 7–11.

Some progress has been achieved on correlations. As mentioned above we do not consider these results to constitute the last word on this delicate and apparently difficult problem.

While we expect that several of these results may constitute useful building stones in a comprehensive description of energy-loss straggling in particular for heavy ions, we emphasize that several important aspects have not been touched upon. Charge-exchange straggling and electron promotion have only been mentioned. The shape of the energy-loss profile – which requires explicit or implicit consideration of higher moments – has not been a topic of the present paper. Finally, problems of experimental geometry have only been mentioned briefly but unquestionably need consideration, *e.g.* along the lines of what has been done in references [43,44] for nuclear stopping.

Thanks are due to Johan Malherbe and Erich Friedland for providing information about their experimental setup. This work has been supported by the Danish Natural Science Research Council (SNF).

References

1. N. Bohr, Philos. Mag. **30**, 581 (1915)
2. N. Bohr, Mat. Fys. Medd. Dan. Vid. Selsk. **18**(8), 1 (1948)
3. P. Sigmund, in *Interaction of Charged Particles with Solids and Surfaces,* edited by A. Gras-Marti, H.M. Urbassek, N. Arista, F. Flores (Plenum Press, New York, 1991), Vol. 271 of NATO ASI Series, pp. 73–144
4. M.S. Livingston, H.A. Bethe, Rev. Mod. Phys. **9**, 245 (1937)
5. J. Lindhard, A.H. Sørensen, Phys. Rev. A **53**, 2443 (1996)
6. L. Flamm, R. Schumann, Ann. Physik **50**, 655 (1916)
7. O. Vollmer, Nucl. Instrum. Meth. **121**, 373 (1974)
8. K.B. Winterbon, Nucl. Instrum. Meth. **144**, 311 (1977)
9. P. Sigmund, Nucl. Instrum. Meth. B **69**, 113 (1992)
10. P. Sigmund, L. Glazov, Nucl. Instrum. Meth. B **136-138**, 47 (1998)
11. L.G. Glazov, P. Sigmund, A. Schinner, Nucl. Instrum. Meth. B **195**, 183 (2002)
12. W.N. Lennard, H. Geissel, D. Phillips, D.P. Jackson, Phys. Rev. Lett. **57**, 318 (1986)
13. E. Bonderup, P. Hvelplund, Phys. Rev. A **4**, 562 (1971)
14. W.K. Chu, Phys. Rev. A **13**, 355 (1976)
15. F. Besenbacher, J.U. Andersen, E. Bonderup, Nucl. Instrum. Meth. **168**, 1 (1980)
16. T. Kaneko, Nucl. Instrum. Meth. B **33**, 151 (1988)
17. P. Sigmund, A. Schinner, Eur. Phys. J. D **12**, 425 (2000)
18. P. Sigmund, A. Schinner, Nucl. Instrum. Meth. B **195**, 64 (2002)
19. P. Sigmund, A. Schinner, in *Fundamental & Applied Aspects of Modern Physics*, edited by S.H. Connell, R. Tegen, (World Scientific, 2001), p. 178
20. N. Bohr, Philos. Mag. **25**, 10 (1913)
21. P. Sigmund, Phys. Rev. A **26**, 2497 (1982)
22. U. Fano, Ann. Rev. Nucl. Sci. **13**, 1 (1963)
23. F. Bloch, Ann. Physik **16**, 285 (1933)
24. H. Bethe, Ann. Physik **5**, 324 (1930)
25. P. Sigmund, Phys. Rev. A **54**, 3113 (1996)
26. P. Sigmund, A. Schinner, Phys. Scripta **T92**, 222 (2001)
27. S. Titeica, Bull. Soc. Roum. Phys. **38**, 81 (1937)
28. P. Sigmund, A. Schinner, Phys. Rev. Lett. **86**, 1486 (2001)
29. P. Hvelplund, Mat. Fys. Medd. Dan. Vid. Selsk. **38**(4), 1 (1971)
30. O.B. Firsov, Sov. Phys. JETP **36**, 1076 (1959)
31. P. Sigmund, A. Fettouhi, A. Schinner, Nucl. Instrum. Meth. B (in press)
32. P. Sigmund, Phys. Rev. A **14**, 996 (1976)
33. P. Sigmund, Ann. Israel Phys. Soc. **1**, 69 (1976)
34. R. Olson, *Atomic, Molecular & Optical Physics Handbook* (Springer, 1996), pp. 664–668
35. N.E.B. Cowern, C.J. Sofield, J.M. Freeman, J.P. Mason, Phys. Rev. A **19**, 111 (1979)
36. J.B. Malherbe, H.W. Albertz, Nucl. Instrum. Meth. **192**, 559 (1982)
37. J.B. Malherbe, H.W. Albertz, Nucl. Instrum. Meth. **196**, 499 (1982)
38. H.H. Andersen, F. Besenbacher, H. Knudsen, Nucl. Instrum. Meth. **149**, 121 (1978)
39. T. Kaneko, Nucl. Instrum. Meth. B **48**, 83 (1990)
40. P. Sigmund, D.-J. Fu, Phys. Rev. A **25**, 1450 (1982)
41. Q. Yang, R.J. MacDonald, Nucl. Instrum. Meth. B **83**, 303 (1993)
42. Q. Yang, Phys. Rev. A **49**, 1089 (1994)
43. B. Fastrup, P. Hvelplund, C.A. Sautter, Mat. Fys. Medd. Dan. Vid. Selsk. **35**(10), 1 (1966)
44. L.G. Glazov, P. Sigmund, Nucl. Instrum. Meth. B (in press)